Vibrational Imaging

DOI: 10.1002/ange.201310725

Live-Cell Quantitative Imaging of Proteome Degradation by Stimulated Raman Scattering**

*Yihui Shen, Fang Xu, Lu Wei, Fanghao Hu, and Wei Min**

Abstract: *Protein degradation is a regulatory process essential to cell viability and its dysfunction is implicated in many diseases, such as aging and neurodegeneration. In this report, stimulated Raman scattering microscopy coupled with metabolic labeling with ^{13}C-phenylalanine is used to visualize protein degradation in living cells with subcellular resolution. We choose the ring breathing modes of endogenous ^{12}C-phenylalanine and incorporated ^{13}C-phenylalanine as protein markers for the original and nascent proteomes, respectively, and the decay of the former wasquantified through $^{12}C/(^{12}C+^{13}C)$ ratio maps. We demonstrate time-dependent imaging of proteomic degradation in mammalian cells under steady-state conditions and various perturbations, including oxidative stress, cell differentiation, and huntingtin protein aggregation.*

Proteins that are abnormal or no longer functioning are actively removed by protein degradation. This degradation is essential to cell viability as a regulatory control in response to physiological and pathological cues.[1] Indeed, disruption of the proteolysis machinery has been implicated in aging and neurodegenerative disorders, in which cells are exposed to the danger of oxidatively damaged proteins or aggregation-prone proteins.[2,3] Extensive efforts have been made to quantify cellular protein degradation. Traditional autoradiography makes use of pulse-chase labeling of radioactive amino acids (e.g., ^{35}S-methionine) combined with treatment with a protein synthesis inhibitor.[4] Later, stable isotope labeling by amino acids in cell culture (SILAC) was developed in tandem with mass spectrometry and works through quantifying the relative amount of "heavy" and "light" peptides.[5–7] However, both of these methods measure the proteome of a collective lysed cell culture and are unable to reveal cell-to-cell or subcellular variation. Even when coupled to secondary ion microscopy in multi-isotope imaging mass spectrometry (MIMS), this invasive detection does not allow live-cell measurement.[8,9] Besides autoradiography and mass spectrometry, fluorescence reporter libraries have enabled proteome half-life determination after a photo-bleach chase.[10] However, this requires the creation of a genomic fusion library and is thus not generally applicable to all cell types.

Herein, we report a general strategy for visualizing the degradation of the overall proteome in living cells with subcellular resolution by coupling metabolic labeling [with ^{13}C-phenylalanine (^{13}C-Phe)] with stimulated Raman scattering (SRS) microscopy. Specifically, we choose the characteristic ring-breathing modes of endogenous ^{12}C-Phe and metabolically incorporated ^{13}C-Phe as the Raman spectroscopic markers for the old and new proteomes, respectively. Proteomic degradation can then be imaged by SRS in living cells through ratio maps of $^{12}C/(^{12}C+^{13}C)$, where the total proteome is represented by the sum of ^{12}C-Phe and ^{13}C-Phe. We demonstrated the utility of our technique by measuring quasi-steady-state proteome degradation in mammalian cell lines and mouse hippocampal neurons, as well as by studying the perturbation caused by oxidative stress, cell differentiation, and protein aggregation. Technically, this is the first time that a ^{13}C-labeled amino acid has been used together with nonlinear vibrational microscopy. Biologically, our proteome imaging method is capable of revealing the global metabolic activity of cells with exquisite spatial resolution.

The choice of phenylalanine as a proteome marker is critical for labeling. First, since it is an essential amino acid that has to be supplied in culture medium, the metabolic incorporation of its ^{13}C isotopologue could distinguish the nascent proteome from the original. Second, its ring-breathing mode exhibits a strong, isolated sharp peak (FWHM $\approx 10\ cm^{-1}$) at $1004\ cm^{-1}$ (Figure 1a, black and Figure S1a in the Supporting Information), thus giving a resolvable shift upon ^{13}C substitution. By contrast, the amide I band (around $1655\ cm^{-1}$) and CH_3 stretching (around $2940\ cm^{-1}$; Figure S1a) as protein markers[11–14] not only give broad bands but also suffer from severe interference from lipids (around $1650\ cm^{-1}$ and $2850\ cm^{-1}$), nucleic acids (around $2950\ cm^{-1}$), and water (around $3100\ cm^{-1}$). Third, compared to the protein-bound phenylalanine concentration of 90 mM,[15] the intracellular free phenylalanine pool (0.5 mM)[16] is essentially negligible. Moreover, since ^{13}C-Phe is supplied in large excess, ^{12}C-Phe from degraded proteins is seldom recycled. In terms of microscopy, the advantage of SRS microscopy (Figure 1b) lies in its superb sensitivity, well-preserved spectra, and linear concentration dependence, thus it is well suited for quantitative live imaging.[13,17–19] Coherent anti-Stokes Raman scattering, another nonlinear microscopy technique, however, has drawbacks such as nonresonant background, spectral distortion, complex concentration dependence, and coherent image artifact.[20]

We first tested the vibrational frequency shift of phenylalanine following ^{13}C labeling. Given that vibration frequency

[*] Y. Shen, F. Xu, L. Wei, F. Hu, Prof. W. Min
Department of Chemistry, Columbia University
New York, NY 10027 (USA)
E-mail: wm2256@columbia.edu
Prof. W. Min
Kavli Institute for Brain Science, Columbia University (USA)

[**] W.M. acknowledges support from National Institutes of Health Director's New Innovator Award and Sloan Research Fellowship.
Supporting information for this article is available on the WWW under http://dx.doi.org/10.1002/anie.201310725.

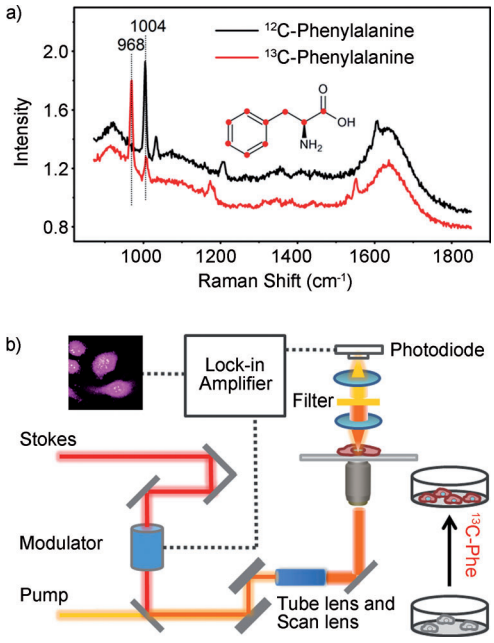

Figure 1. ^{13}C-Phe labeling combined with SRS microscopy. a) Spontaneous Raman spectra of ^{12}C-Phe (black) and ^{13}C-Phe (red) showing the vibrational frequency shift from 1004 cm^{-1} to 968 cm^{-1}. Inset: the structure of phenylalanine with the ^{13}C sites indicated by red dots. b) The experimental setup of SRS microscopy.

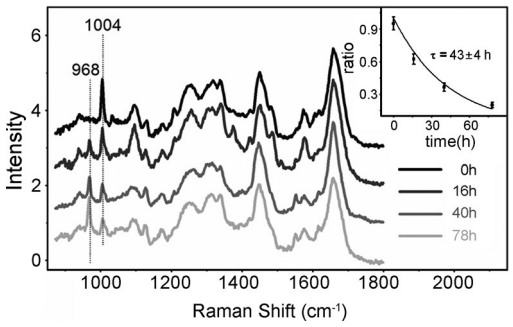

Figure 2. Time-dependent spontaneous Raman spectra of HeLa cells with 80 s acquisition, showing a decline in the 1004 cm^{-1} peak and a rise in the 968 cm^{-1} peak. The valley at 986 cm^{-1} is used in background subtraction for the SRS images. Inset: single exponential fitting of the ^{12}C/(^{12}C+^{13}C) ratios obtained from the spectra.

is inversely proportional to the square root of reduced mass, and also taking H atoms into account, the Raman peak of uniformly ^{13}C-labeled phenylalanine (i.e., ^{13}C-Phe) should red shift to $1004 \times \sqrt{13/14} = 967.5$ cm^{-1}, which is close to the measured 968 cm^{-1} in buffer solution (Figure 1a, red). This peak shift has also been observed in microbes fed with ^{13}C-glucose.[21] Some attention needs to be paid to the signal extraction because both ^{12}C- and ^{13}C-Phe Raman peaks sit on a flat baseline (950–1050 cm^{-1}; Figure S1a). Since SRS preserves spontaneous Raman spectra (Figure S1b), we adopt a simple and robust subtraction strategy to determine the net phenylalanine signal: using the central valley at 986 cm^{-1} to represent the baseline background, and then subtracting it from images at the two peaks (968 cm^{-1} and 1004 cm^{-1}). We notice that there is a smaller peak from ^{13}C-Phe overlapping with the 1004 cm^{-1} peak of ^{12}C-Phe. After treating this as a linear contribution from the ^{13}C channel to the ^{12}C channel with a coefficient of 0.14, we can obtain pure ^{13}C and ^{12}C signals as $I(^{13}C) = I_{968} - I_{986}$ and $I(^{12}C) = I_{1004} - I_{986} - 0.14\,I(^{13}C)$, where I represents the intensity from the spectrum or image.

We then demonstrated our method in cultured HeLa cells. After the cells were incubated with 0.8 mM ^{13}C-Phe substituted medium, time dependent spontaneous Raman spectra were measured from fixed cells (Figure 2). The endogenous ^{12}C peak shows an apparent decay while the ^{13}C peak increases over time, thus proving the success of metabolic incorporation. The normalized ratios [^{12}C/(^{12}C+^{13}C)] over time were fitted to an exponential decay ($\tau = 43 \pm 4$ h; Figure 2, inset). To obtain ratio maps, we set up the SRS microscope as previously described (Figure 1b and the Supporting Information).[11] Live cell SRS images were acquired at 3 Raman shifts (968 cm^{-1}, 986 cm^{-1}, 1004 cm^{-1}; Figure S2). After background subtraction, gradual weakening of the resulting ^{12}C channels clearly indicates the degradation of the old proteome (Figure 3a). As expected, the amount of total proteome remains almost unchanged under quasi-steady-state conditions, as confirmed by the sum images from the ^{12}C and ^{13}C channels (Figure S2). Ratio maps were

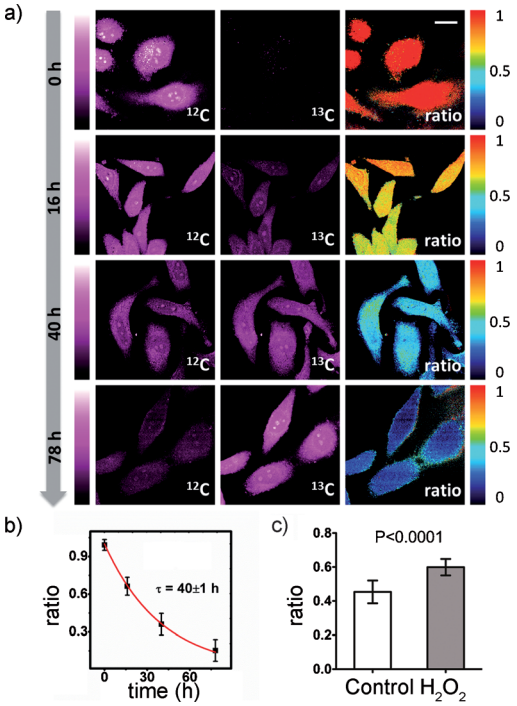

Figure 3. SRS images reveal protein degradation kinetics in HeLa cells. a) Background-subtracted SRS images and ^{12}C/(^{12}C+^{13}C) ratio maps of HeLa cells show obvious decay in the ^{12}C channel and increase in the ^{13}C channel over time. Ratio images show decay from ≈1.0 to ≈0.2. Scale bar: 20 μm. b) Single exponential fitting of the ^{12}C/(^{12}C+^{13}C) ratios obtained from the SRS images. Error bar: standard deviation. c) Treatment with H_2O_2 results in a slower degradation in HeLa cells incubated with ^{13}C-Phe for 24 h. Control: ratio = 0.45 ± 0.07, n = 12; H_2O_2 treated: ratio = 0.60 ± 0.05, n = 14, where n is number of cells analyzed.

calculated as normalized $^{12}C/(^{12}C+^{13}C)$ to account for cell-to-cell variation and laser power fluctuation. One can readily infer how fast the degradation is from these ratio maps. To compare our results with the results from collective cell culture, we fitted averaged ratios with single exponential decay ($\tau = 40 \pm 1$ h; Figure 3b). This is close to what was determined earlier from the spectra and also matches the 35 h reported from mass spectrometry.[22]

We also examined the effect of oxidative stress on protein turnover. Reactive oxygen species (ROS) production and cellular antioxidant defense are normally balanced as part of homeostasis. However, under severe oxidative stress, accumulation of ROS will harm the proteolysis machinery, thus retarding protein degradation.[2,23] We measured proteomic degradation in HeLa cells treated with 200 μM H_2O_2 through 24 h ^{13}C-Phe labeling. Cells treated with H_2O_2 exhibit a ^{12}C ratio approximately 25% higher than the control cells, thus indicating slower protein degradation under oxidative stress (Figure 3c).

Our technique could readily be applied to study protein degradation in other cell lines or primary cells under either steady state or differentiation conditions. For example, in live HEK293T cells (Figure S3), protein degradation was found to follow similar decay patterns but exhibited faster kinetics ($\tau = 33 \pm 3$ h, Figure S4). This is consistent with the fact that these cells grow faster than HeLa cells. We went on to demonstrate the technique in primary mouse hippocampal neuron culture (Figure S5a) by using the same concentration of ^{13}C-Phe. Protein degradation clearly takes place after 24 h, but much more slowly (Figure S5b), a result consistent with the profound metabolic difference between neurons (post-mitotic) and HeLa or HEK293T cells (immortalized). We further obtained SRS images during PC12 cell differentiation induced by NGF-β in the presence of ^{13}C-Phe (Figure 4). The results reveal protein degradation kinetics with $\tau = 48 \pm 10$ h (Figure S4).

Finally we studied the impact of protein aggregation on proteomic degradation with subcellular resolution. It is generally believed that polyQ expansion is one of the genetic reasons for neurodegenerative disorders such as Huntington's disease.[24] Overexpression of mutant huntingtin (Htt) could overwhelm the capacity of cellular proteolysis and lead to the formation of aggregates as inclusion bodies (IBs). However, the precise role of aggregate formation is still under debate. We expressed a fluorescent protein (mEos2)-tagged N-terminal fragment of the mutant huntingtin protein, mEos2-Htt-Q94, in HEK293T cells as a protein aggregation model. 24 hrs after plasmid transfection, the cells were switched to ^{13}C-Phe medium and imaged 24 h and 48 h later (Figure 5a and the Supporting Information). mEos2 fluorescence images revealed bright cluster regions corresponding to IBs. The same regions in the ratio maps (Figure 5b, arrow) show severely retarded degradation, thus confirming impaired proteolysis inside IBs. The subcellular mapping capability of our technique was indispensable to resolving this compartmentalized impairment of metabolic activity. We noticed that interference in the SRS signal from the two-photon absorption of mEos2 was a possibility. To exclude this, we photobleached mEos2 and restored the SRS images (data not shown). We also used a non-chromophore sequence, SNAP-Htt-Q94, to transfect HEK293T cells and this led to results similar to those obtained with mEos2-Htt-Q94 (Figure S6).

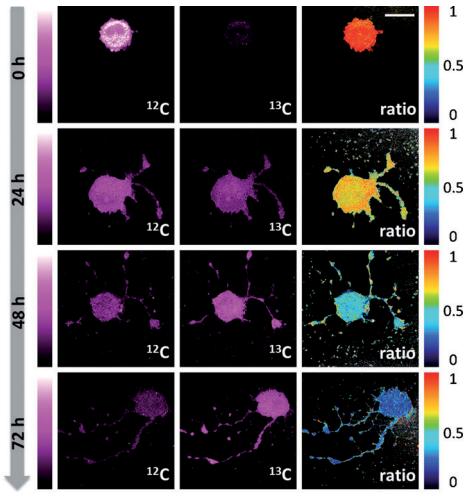

Figure 4. SRS images reveal protein degradation during PC12 differentiation induced by NGF-β. Scale bars: 20 μm.

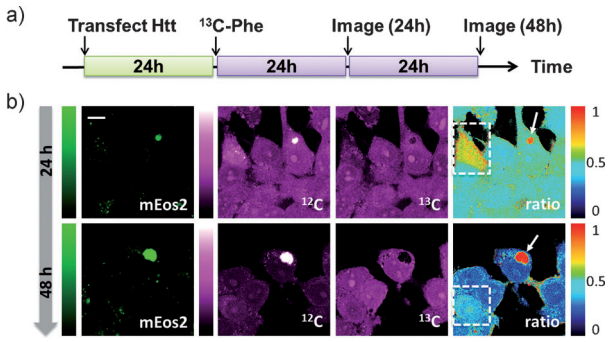

Figure 5. Proteomic degradation in HEK293T cells during Htt-Q94 aggregation. a) Experimental timeline. b) First column: mEos2 fluorescence images indicate the formation of IBs. Second and third columns: SRS images from the ^{12}C and ^{13}C channels, respectively. Last column: SRS $^{12}C/(^{12}C+^{13}C)$ ratio maps with subcellular resolution reveal retarded degradation inside inclusion bodies (arrow) as well as a pronounced slowing of cytoplasmic protein degradation within a few cells (box). Scale bar: 10 μm.

Remarkable cell-to-cell variations were observed, thus shedding light on the functional role of IB formation. While the degradation rates for cytoplasmic proteins in most tested cells were very similar to those of non-transfected cells (Figure S3), there were a few that exhibited markedly slower degradation (hotter colors; Figure 5b, box). Interestingly, these cells showed only diffusive Htt-Q94 (or small IBs) in their fluorescence images. By contrast, the cells containing large IBs displayed normal degradation rates for the cytoplasmic proteins. Hence, our observation lends support to the emerging hypothesis that the diffusive oligomers of aggregation-prone proteins might become toxic to cells by gradually interfering with the proteasome machinery, while the forma-

tion of inclusion bodies may actually play a neuroprotective role by sequestering the diffusive toxic species.[25,26]

In summary, we demonstrated the coupling of SRS microscopy with ^{13}C-Phe labeling in quantitative imaging of protein degradation. Compared to existing approaches, our method is unique in several aspects. First, the stable ^{13}C isotope introduces minimal perturbation; meanwhile SRS offers noninvasive detection with subcellular resolution. Neither autoradiography nor mass spectrometry can be used to probe living cells. Second, the intrinsic contrast of ^{12}C-Phe offers an endogenous marker for the preexisting proteome. This is not achievable for bioorthogonal alkyne tagging,[27–29] which can only be used to visualize the newly incorporated tags. Likewise, the recently reported deuterium labeling approach allows imaging only of proteome synthesis and not degradation[11] (note that monitoring the decay of the C–D signal after pulse-chase with deuterated amino acids would not work since the C–D signal would gradually transfer from proteins to other metabolites such as lipids[30]). Finally, unlike analysis of individual proteins, our proteomic approach reveals global proteolysis activity, a phenotype in many diseases, thus our technique can be applied to drug screening when the proteolysis state of the cells is a key functional readout.

Received: December 10, 2013
Published online: April 15, 2014

Keywords: isotope labeling · protein aggregation · protein degradation · Raman spectroscopy · SRS microscopy

[1] A. L. Goldberg, *Nature* **2003**, *426*, 895 – 899.
[2] R. Shringarpure, K. Davis, *Free Radical Biol. Med.* **2002**, *32*, 1084 – 1089.
[3] A. Tsvetkov, M. Arrasate, S. Barmada, *Nat. Chem. Biol.* **2013**, *9*, 586 – 592.
[4] A. Bachmair, D. Finley, A. Varshavsky, *Science* **1986**, *234*, 179 – 186.
[5] M. Mann, *Nat. Rev. Mol. Cell Biol.* **2006**, *7*, 952 – 958.
[6] M. Larance, Y. Ahmad, K. J. Kirkwood, T. Ly, A. I. Lamond, *Mol. Cell. Proteomics* **2013**, *12*, 638 – 650.
[7] M. K. Doherty, D. E. Hammond, M. J. Clague, S. J. Gaskell, R. J. Beynon, *J. Proteome Res.* **2009**, *8*, 104 – 112.
[8] D.-S. Zhang, V. Piazza, B. J. Perrin, A. K. Rzadzinska, J. C. Poczatek, M. Wang, H. M. Prosser, J. M. Ervasti, D. P. Corey, C. P. Lechene, *Nature* **2012**, *481*, 520 – 524.
[9] M. L. Steinhauser, A. P. Bailey, S. E. Senyo, C. Guillermier, T. S. Perlstein, A. P. Gould, R. T. Lee, C. P. Lechene, *Nature* **2012**, *481*, 516 – 519.
[10] E. Eden, N. Geva-Zatorsky, I. Issaeva, A. Cohen, E. Dekel, T. Danon, L. Cohen, A. Mayo, U. Alon, *Science* **2011**, *331*, 764 – 768.
[11] L. Wei, Y. Yu, Y. Shen, M. C. Wang, W. Min, *Proc. Natl. Acad. Sci. USA* **2013**, *110*, 11226 – 11231.
[12] D. Zhang, P. Wang, M. N. Slipchenko, D. Ben-Amotz, A. M. Weiner, J.-X. Cheng, *Anal. Chem.* **2013**, *85*, 98 – 106.
[13] Y. Ozeki, W. Umemura, Y. Otsuka, S. Satoh, H. Hashimoto, K. Sumimura, N. Nishizawa, K. Fukui, K. Itoh, *Nat. Photonics* **2012**, *6*, 845 – 851.
[14] X. Zhang, M. B. J. Roeffaers, S. Basu, J. R. Daniele, D. Fu, C. W. Freudiger, G. R. Holtom, X. S. Xie, *ChemPhysChem* **2012**, *13*, 1054 – 1059.
[15] H.-J. van Manen, A. Lenferink, C. Otto, *Anal. Chem.* **2008**, *80*, 9576 – 9582.
[16] K. Piez, H. Eagle, *J. Biol. Chem.* **1958**, *231*, 533 – 545.
[17] C. W. Freudiger, W. Min, B. G. Saar, S. Lu, G. R. Holtom, C. He, J. C. Tsai, J. X. Kang, X. S. Xie, *Science* **2008**, *322*, 1857 – 1861.
[18] B. G. Saar, C. W. Freudiger, J. Reichman, C. M. Stanley, G. R. Holtom, X. S. Xie, *Science* **2010**, *330*, 1368 – 1370.
[19] P. Wang, J. Li, P. Wang, C.-R. Hu, D. Zhang, M. Sturek, J.-X. Cheng, *Angew. Chem.* **2013**, *125*, 13280 – 13284; *Angew. Chem. Int. Ed.* **2013**, *52*, 13042 – 13046.
[20] W. Min, C. W. Freudiger, S. Lu, X. S. Xie, *Annu. Rev. Phys. Chem.* **2011**, *62*, 507 – 530.
[21] H. N. Noothalapati Venkata, S. Shigeto, *Chem. Biol.* **2012**, *19*, 1373 – 1380.
[22] S. B. Cambridge, F. Gnad, C. Nguyen, J. L. Bermejo, M. Krüger, M. Mann, *J. Proteome Res.* **2011**, *10*, 5275 – 5284.
[23] N. Breusing, T. Grune, *Biol. Chem.* **2008**, *389*, 203 – 209.
[24] H. Y. Zoghbi, H. T. Orr, *Annu. Rev. Neurosci.* **2000**, *23*, 217 – 247.
[25] M. Arrasate, S. Mitra, E. S. Schweitzer, M. R. Segal, S. Finkbeiner, *Nature* **2004**, *431*, 805 – 810.
[26] J. Tyedmers, A. Mogk, B. Bukau, *Nat. Rev. Mol. Cell Biol.* **2010**, *11*, 777 – 788.
[27] D. C. Dieterich, J. J. L. Hodas, G. Gouzer, I. Y. Shadrin, J. T. Ngo, A. Triller, D. a Tirrell, E. M. Schuman, *Nat. Neurosci.* **2010**, *13*, 897 – 905.
[28] L. Wei, F. Hu, Y. Shen, Z. Chen, Y. Yu, C.-C. Lin, M. C. Wang, W. Min, *Nat. Methods* **2014**, *11*, 410 – 412.
[29] L. Lin, X. Tian, S. Hong, P. Dai, Q. You, R. Wang, L. Feng, C. Xie, Z.-Q. Tian, X. Chen, *Angew. Chem.* **2013**, *125*, 7407 – 7412; *Angew. Chem. Int. Ed.* **2013**, *52*, 7266 – 7271.
[30] F. Hu, L. Wei, C. Zheng, Y. Shen, W. Min, *Analyst* **2014**, DOI: 10.1039/c3an02281a.

